

# Scene-Conditional 3D Object Stylization and Composition

Jinghao Zhou   Tomas Jakab   Philip Torr   Christian Rupprecht  
 University of Oxford  
 {jinghao,tomj,chrisr}@robots.ox.ac.uk  
[shallowtoil.github.io/scene-cond-3d](https://github.com/shallowtoil/scene-cond-3d)

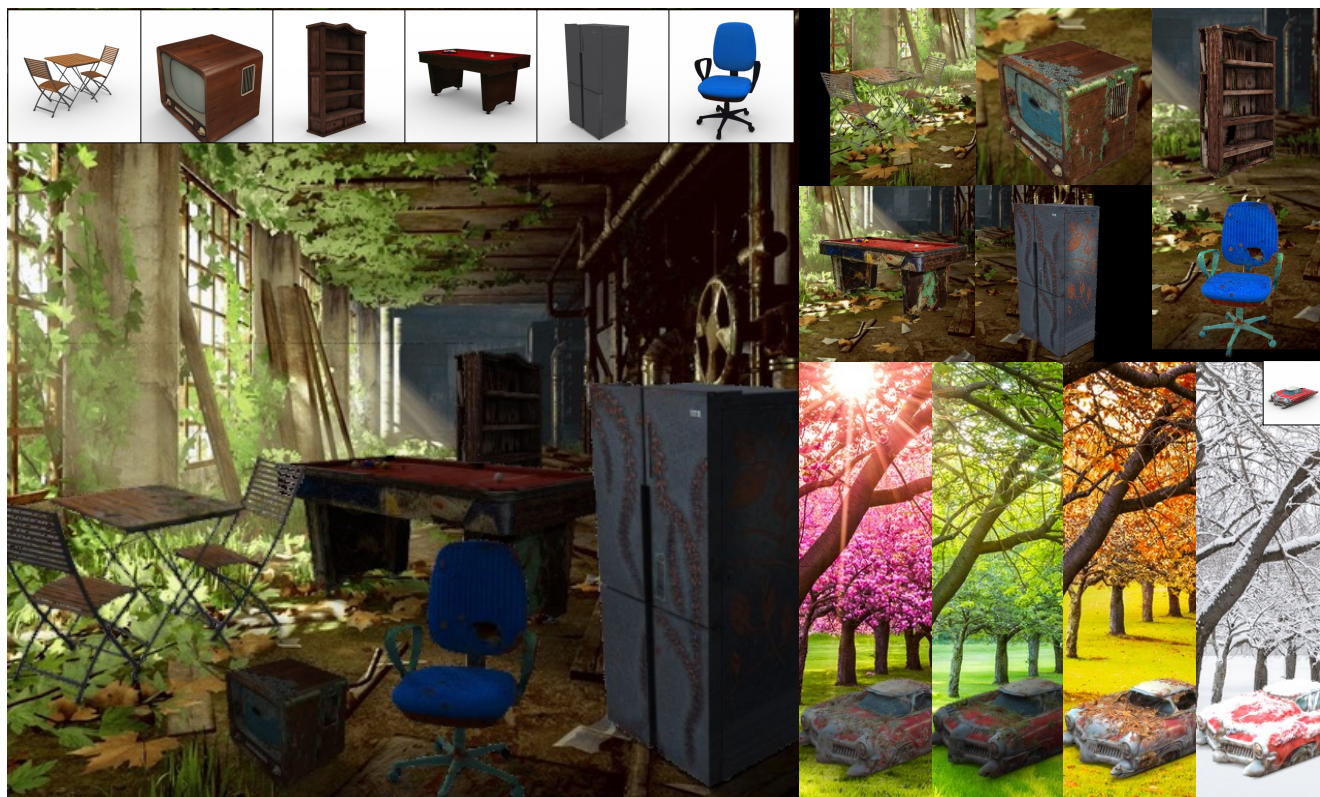


Figure 1. We present a framework that adapts a 3D object’s appearance to a location in a 2D scene. It creates an image where the 3D object is seamlessly blended (left & bottom right), with its appearance influenced by the scene’s environmental conditions and lighting effects. Moreover, the stylized object with adapted textures (top right), rendered here without the estimated lighting condition for illustrative purposes, can be further utilized as 3D assets for downstream tasks such as video games.

## Abstract

Recently, 3D generative models have made impressive progress, enabling the generation of almost arbitrary 3D assets from text or image inputs. However, these approaches generate objects in isolation without any consideration for the scene where they will eventually be placed. In this paper, we propose a framework that allows for the stylization of an existing 3D asset to fit into a given 2D scene, and additionally produce a photorealistic composition as if the asset

was placed within the environment. This not only opens up a new level of control for object stylization, for example, the same assets can be stylized to reflect changes in the environment, such as summer to winter or fantasy versus futuristic settings—but also makes the object-scene composition more controllable. We achieve this by combining modeling and optimizing the object’s texture and environmental lighting through differentiable ray tracing with image priors from pre-trained text-to-image diffusion models. We demonstrate that our method is applicable to a wide variety of indoor

and outdoor scenes and arbitrary objects.

## 1. Introduction

After the success of generative models [22, 46, 49] for images in computer vision, the community is now interested in lifting these models to 3D [43, 58] through advances in architectures, data, and training. These lifted 3D models demonstrate relatively plausible 3D representations of objects conditioned on images or texts.

While generating whole objects—*e.g.* *an astronaut riding a horse*—is a challenging problem that generative models are becoming able to solve, in practice, these assets are difficult to adapt for use in downstream applications or existing virtual environments such as video games because they are generated without context.

In this paper, we aim to provide a mechanism to close the appearance gap between 3D objects and environments. We formulate this problem through the lens of a creative tool. The intended goal of this paper is to align the appearance of a 3D object to a customized 2D scene as we place it into a specific location, a challenging task that requires fine-grained visual control for convincing results.

We are interested in producing a photorealistic scene-object composition where the 3D object is seamlessly blended. For instance, an object placed in a rainy night scene should appear wet and dimly lit, and if the scene is muddy and sunny, the object should also look muddy and cast a strong shadow. To achieve a high level of realism on a fine-grained level, the mud on the object must match the scene’s mud in appearance and the direction of the shadow must match where the sun is located. Instead of simply resorting to 2D blending operations [20, 54], we explicitly model an object’s appearance and lighting in 3D space, which enables more accurate and regularized control of the object’s appearance in the composed image.

We also aim to preserve the underlying object geometry and appearance factors not related to the scene environment. This task is highly practical; for example, for media design, when presenting a 3D asset of a product within a realistic scene, we want the product to blend naturally while remaining recognizable. Manually achieving this would require a skilled artist to modify the object’s texture to match the scene, a process that is both challenging and time-consuming. Our paper introduces a method that automates this task. It accepts a 3D object with texture, a 2D scene, and the object’s position within the scene, and outputs an adapted texture that is consistent with the scene.

To accomplish this, we leverage recent advances in generative diffusion models [49, 50] for images, which are trained on a large-scale dataset of internet images. We conduct an optimization procedure where we compose the 2D renderings of the 3D object with the 2D scene at a specified

location and use a pre-trained diffusion model to “critique” the realism of the composed image, providing a gradient signal for optimization.

The challenge with this is that diffusion models, such as Stable Diffusion [49], are trained on 2D images and lack any notion of 3D geometry. Naively optimizing or denoising in 2D space [20, 54] would result in the loss of the object’s 3D geometry. To prevent this, we optimize the object’s content in 3D by randomly rotating the object during optimization and rendering it from various viewpoints, which helps to align the adapted texture with the object’s geometry and avoid overfitting to a single viewpoint.

Notably, randomly rotating the 3D object stops lighting effects from being baked into the texture which is desirable but it also prevents the object from naturally blending with the scene in a single viewpoint. To counteract this, we predict the scene’s lighting and the shadows cast by the object as separate components. For this purpose, we propose a novel technique inspired by a common physical approach from the computer graphics industry, where reflective and diffuse spheres with known material parameters are placed and photographed in a real-world scene to capture the environmental lighting conditions. We adopt this concept and place a virtual white diffuse sphere inside the scene during optimization while conditioning the generative model to expect a white sphere within the scene, thereby capturing the model’s interpretation of the scene’s lighting in a form that can be easily extracted.

Optimizing the object’s appearance in 3D offers further significant advantages: The user can change the object’s pose without re-running the optimization, as the texture is meaningful from all viewpoints, and view-dependent effects are modeled separately by the lighting component. Additionally, the 3D object with the adapted texture can be used as a standalone asset in other downstream tasks (*e.g.* in a video game).

In summary, we present a framework that (1) enables the stylization of a 3D object, which can also be used as a standalone asset, given a 2D scene and its location within it; (2) achieves photorealistic scene-object compositing with the help of a novel mechanism to estimate scene lighting from a single image.

We further verify the effectiveness of our method in extensive experiments, demonstrating that our approach can realistically adapt objects to a diverse set of environments, laying the groundwork for practical applications.

## 2. Related Work

The purpose of this paper is to adapt the appearance of a 3D object to align with a customized 2D scene. This solves a more complicated problem than prior works, which often only tackle individual components, including but not limited to 2D scene-object compositing, light estimation, and

Method	Scene			Object			Compose	
	Rep.	Lighting	Shadow	Rep.	Appearance	Env. Inf.		I.D. Pre.
OST [54]	<input type="checkbox"/>	-	✓	<input type="checkbox"/>	-	✓	✓	Blend
CDC [20]	<input type="checkbox"/>	Amb. ❄️	✓	<input type="checkbox"/>	Diff. ❄️	✓	✓	Blend
IGAN [31]	<input type="checkbox"/>	LDR 💧	✓	<input type="checkbox"/>	Diff. ❄️	✗	✗	C & P
EVL [30]	<input type="checkbox"/>	HDR 💧	✓	<input type="checkbox"/>	Diff. ❄️	✗	✗	C & P
PrDr [59]	-	Amb. ❄️	✗	<input type="checkbox"/>	Diff. 🔥	✓	✗	-
Fan3D [7]	-	HDR ❄️	✗	<input type="checkbox"/>	PBR 🔥	✓	✗	-
Inst3D [29]	-	Point ❄️	✗	<input type="checkbox"/>	Diff. 🔥	✓	✓	-
<b>Ours</b>	<input type="checkbox"/>	HDR 🔥	✓	<input type="checkbox"/>	PBR 🔥	✓	✓	C & P

Table 1. **Comparison with related work.** *Rep.* denotes representation by 2D () or 3D (). *Env. Inf.* denotes *Environmental Influence* and *I.D. Pre.* denotes *Identity Preservation*. Parameters for the lighting and the appearance model are either scene-agnostic constant (❄️), scene-conditioned predictable (💧), or learnable (🔥). Amb. denotes an ambient light source. Diff. denotes a purely diffuse appearance. C & P denotes copy-and-paste.

texturing, but never as a whole. We compare with these methods next and detail their differences in Tab. 1.

**Scene-Object Compositing.** Scene-object compositing is a challenging task that requires a delicate balance between visual transfer and control. It has been extensively researched [5, 8, 9, 28]. Recent methods condition the denoising process of diffusion models [22, 53] on object images. OST [54] aims to seamlessly integrate a 2D object image into a 2D scene by modifying the keys and values in the attention blocks. CDC [20] considers composing the 2D renderings of a 3D object with a 2D scene by directly modifying denoised latent.

However, these methods rely entirely on the 2D denoising process and do not explicitly model the object’s geometry, which often results in a significant loss of the object’s structural details and identity. The limitation severely hampers these methods’ ability to adapt to the environmental and lighting conditions of the scene.

**Light Estimation from Single-View Image.** Estimating light conditions from a single-view 2D image is of practical use in the real world and has been extensively studied for both indoor [16, 17] and outdoor scenes [24, 25, 63]. The distinction between these two settings has been significantly narrowed recently [30, 31], thanks to the outperforming capabilities of diffusion models, which have contributed to a unified framework. With additional training on large high dynamic range (HDR) datasets such as SUN360 [61], these methods can approximate the location and intensity of the light source, enabling the generation of realistic shadows.

However, these methods estimate only the lighting of the scene. They are typically indifferent to how objects should

be stylized to match the scene, neglecting the potential environmental influences on the textures of objects.

**Mesh Texturing.** Classic automated approaches [60] for mesh texturing are often limited and apply only simple texture patterns. In contrast, methods [15, 40, 52] based on Generative Adversarial Networks [18] (GANs) are more capable of synthesizing detailed textures. Recently, text-conditioned texture generation [37, 38] has been made possible through the optimization of CLIP-based objectives [45]. The latest works now employ powerful text-to-image diffusion models [22, 53], either through optimization [7, 32, 36, 55, 59] using Score Distillation Sampling [43] (SDS), or by wrapping the generated 2D textures onto the mesh [4, 6, 48]. Importantly, Variational Score Distillation [59] (VSD) as an improved optimization objective and the adoption of PBR model [7] have greatly boosted the quality of generated textures. Additionally, an increasing level of requirement for more visual control from users has been partially met [21, 29] through image-conditional diffusion models [3] to preserve objects’ identities.

However, these works focus on texturing the object in isolation from the scene and do not consider the homogeneity of the composition when these assets are placed in certain environments, which limits their practical usage.

### 3. Method

The overall structure of our framework can be found in Fig. 2. Given a textured 3D object, a 2D image of a scene, and a 2D location where to place the object, we first adapt the texture of the 3D object (Sec. 3.2) to align with the scene. To enable a photorealistic composition of the object and the scene, we further estimate the lighting of the scene (Sec. 3.3) and apply it during the final rendering.

#### 3.1. Optimization

To enable end-to-end optimization, we adopt a differentiable renderer to render the object and score it using the priors from diffusion models.

**Differentiable Renderer.** We employ the differential renderer Mitsuba3 [26] (denoted as  $g$ ), due to its capabilities as a physically-based ray-tracing renderer equipped with versatile rendering options, such as diverse BSDFs, the path tracer integrator, and using an environment map as a light source. This enables us to produce photo-realistic renders complete with shadows and reflections, forming the foundation for robust texture adaptation and light estimation.

**Diffusion Model as Guidance.** To score the rendered image, we make use of a generative diffusion model [49, 50]  $\phi$ . Diffusion models have learned powerful priors of the image formation process in the real world from large-scale training on billion-scale web data. Similar to prior work [43, 58], we supervise the rendered image  $x_0 = g(\theta)$  with a score-

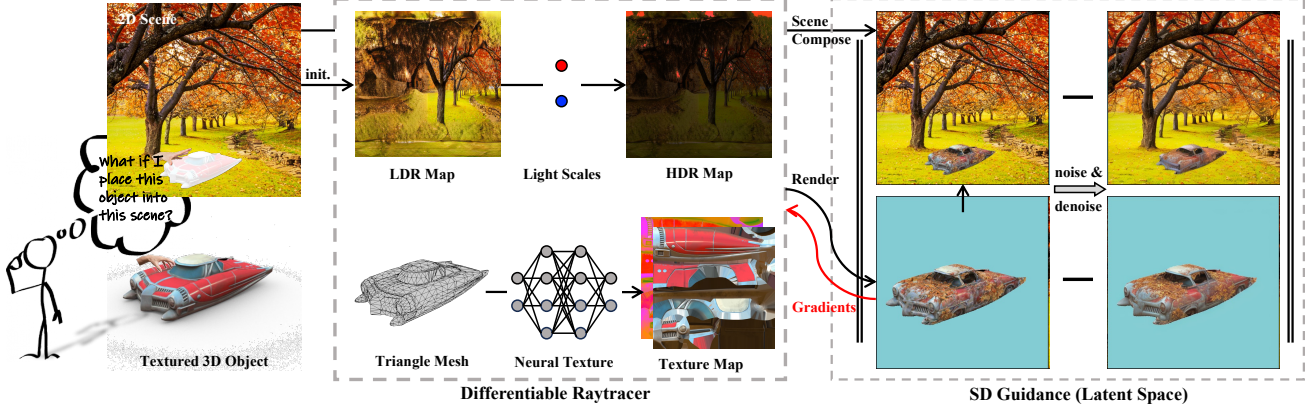


Figure 2. **Framework.** We learn environment map and texture map *separately* from the 2D supervision. We initialize (*init.*) the environment map with an LDR map estimated from the 2D scene and learn light multiplying scales bright areas, yielding an HDR map. We employ the PBR material model for texture maps, encoded via MLP with positional encoding. The object is rendered through a differentiable raytracer and further composed with the scene background, receiving gradients from Stable Diffusion (SD) in the latent space.

matching objective to obtain an image gradient

$$\nabla_{\theta} \mathcal{L}(\mathbf{x}_0) \triangleq \mathbb{E}_{t, \epsilon} \left[ w_t (\epsilon_{\phi}(\mathbf{x}_t) - \hat{\epsilon}(\mathbf{x}_t)) \frac{\partial \mathbf{x}_0}{\partial \theta} \right], \quad (1)$$

where  $\mathbf{x}_t = \sqrt{\alpha_t} \mathbf{x}_0 + \sqrt{1 - \alpha_t} \epsilon$  is the noisy rendered image,  $\epsilon_{\phi}(\mathbf{x}_t)$  is an approximated score for a noisy real image,  $t \in \mathbb{N}$  indexes the discrete diffusion steps, and  $\hat{\epsilon}$  is a scoring function for  $\mathbf{x}_t$ . Specifically,  $\hat{\epsilon}$  is set as constant  $\epsilon$  in Score Distillation Sampling [43] (SDS), and  $\epsilon_{\psi}$  is an online LoRA-tuned network initialized from  $\epsilon_{\phi}$  in Variational Score Sampling [59] (VSD). Notably, we employ their interpolated variant given by  $\hat{\epsilon} = \lambda \epsilon_{\psi} + (1 - \lambda) \epsilon$  with a  $\lambda$  annealed from 1 to  $\lambda_e$ , helping to counteract the over-texturization often observed in VSD, especially for objects with simple surfaces. With residual of noises  $\epsilon_{\phi} - \hat{\epsilon} = (\epsilon_{\phi} - \epsilon) - \lambda(\epsilon_{\phi} - \epsilon_{\psi})$ , we highlight its relation with the image gradient obtained in traditional inverse rendering setup  $\nabla_{\theta} \mathcal{L}(\mathbf{x}_0) = \mathbf{x}_0 - \mathbf{x}_{\text{gt}}$  by reformulating it as

$$\epsilon_{\phi} - \hat{\epsilon} = \sqrt{\frac{\alpha_t}{1 - \alpha_t}} [(\mathbf{x}_0 - \hat{\mathbf{x}}_{\phi}) - \lambda(\mathbf{x}_0 - \hat{\mathbf{x}}_{\psi})], \quad (2)$$

where the target used to supervise  $\mathbf{x}_0$  is predicted clean image  $\hat{\mathbf{x}}_{\phi}$  from  $\epsilon_{\phi}$  as the positive and  $\hat{\mathbf{x}}_{\psi}$  from  $\epsilon_{\psi}$  as the negative. The technique enables nominal classifier-free guidance [23] and thus bypasses mode-seeking behaviors and saturated texture. Inspired by [48], we incorporate the inner product of the camera pose and object’s surface normal  $\langle \mathbf{c}, \mathbf{n} \rangle$  into  $w_t$  to penalize faces at small grazing angles. In practice, we use Stable Diffusion [49] (SD) and absorb the encoder into  $g$ , optimizing in latent space.

## 3.2. Texture Adaptation

### 3.2.1 Appearance Model

**Textured Mesh.** We represent the 3D object as a textured mesh, which is the most common format for 3D assets in

the industry and is compatible with many established workflows. Textured meshes are available in abundance in online datasets and marketplaces [1, 10], and recently, one can also generate reasonable quality 3D meshes with text descriptions [7, 32, 59] or limited viewpoints [33, 44].

**Neural Texture.** We represent the appearance of objects using a texture map  $\mathcal{T} \in \mathbb{R}^{H_t \times W_t \times 5}$ , facilitating compatibility of textured results with widely-used rendering engines, such as Blender. We parameterize the texture using a coordinate neural network that maps 3D coordinates to the texture attributes. We first map the 3D coordinates of vertices using a rasterizer [39] based on to their UV coordinates into the space of the texture map, resulting in  $\mathcal{C} \in \mathbb{R}^{H_t \times W_t \times 3}$ . We then use a 2-layer parameterized MLP without bias and Hash positional encoding  $\Phi : \mathcal{C} \rightarrow \mathcal{T}$  to map the coordinates to their texture attributes. For the final layer, we re-map the output activated after sigmoid according to pre-defined minimal and maximal values. The five channels in  $\mathcal{T}$  correspond to the Physically-Based Rendering (PBR) shading model [35], which includes a diffuse term  $k_d \in \mathbb{R}^3$  and an isotropic specular GGX lobe [57] described by  $k_{\text{rm}} = (k_r, k_m) \in \mathbb{R}^2$ , with  $k_r$  representing roughness and  $k_m$  indicating metalness. The PBR model, with  $k_r$  affecting the scattering of light and  $k_m$  influencing the reflective properties, creates a realistic representation of how light interacts with surfaces.

### 3.2.2 Scene-Conditional Guidance

Achieving a realistic texture adaptation for 3D objects placed into 2D scenes requires three components: *Environmental Influence* involves adjusting the texture to realistically reflect the environmental impact; *Identity Preservation* aims to preserve the objects’ unique visual aspects, and *Blending* focuses on guiding the texture adaptation to match the visual characteristic of the scene, ensuring seam-

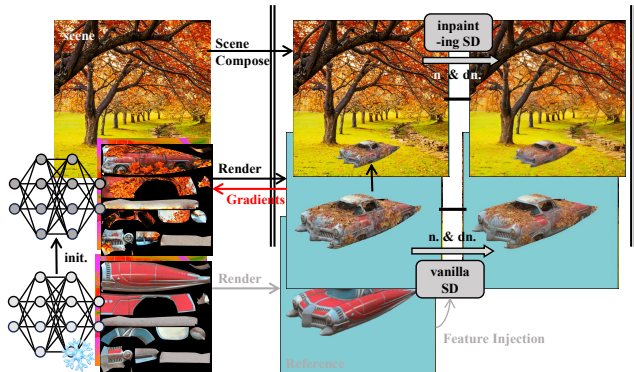


Figure 3. **Pipeline for texture adaptation.** We initialize (*init.*) the neural texture from the reference object and inject the feature of reference renderings to the U-Net of SD. We use both *local-view* and *global-view* guidance. *n.* & *dn.* denotes noise and denoise.

less integration with the surroundings and avoiding stark contrasts.

**Environmental Influence.** To show the realistic effects of the scene environment on the object’s appearance, we guide the diffusion model with text prompts. We find that a naive text prompt, combining a simple object description with a scene description, *e.g.*, *a leather sofa in a swamp*, is insufficient to generate realistic textures that reflect the environmental impact on the object, as shown in the appendix. For instance, we would expect a sofa placed in a swamp to have a dirty appearance and possibly show signs of moss or other vegetation growth. Instead of manually crafting a detailed text prompt for each object and scene combination, we automatize the process by employing a large language model (LLM), specifically GPT-4 [41], to generate a text prompt for the image diffusion model. Given the simple description of the object (*e.g.*, *a leather sofa*) and the scene (*e.g.*, *a swamp*), we instruct the LLM to first analyze the potential impact of the scene’s environment on the object’s appearance and then to distill this information into a text prompt that describes the resulting appearance of the object (*e.g.*, *The leather sofa, partially submerged in the swamp, looks discolored and soggy, its once-polished surface marred by mud, moss, and the murky water of the swamp environment.*). We then use this automatically generated text prompt to guide the diffusion model in adapting the texture. The specific prompt design for this automated process is detailed in the appendix.

**Identity Preservation.** To prevent the transferred texture from drifting away from its original content, we regularize the denoising diffusion model with reference images, a technique that has been explored for controlled image generation [42, 56]. Suppose we have a rendered reference image  $\mathbf{x}_0^r = g(\theta^r)$  and its noised version  $\mathbf{x}_t^r$  as input forwarded to  $\epsilon_\phi$  and  $\epsilon_\psi$ , for the Multi-Head Self-Attention (MHSA) layer in each Transformer block of  $\epsilon_\phi$ ’s and  $\epsilon_\psi$ ’s U-Nets, we concatenate the key  $K^r$  and value  $V^r$  of  $\mathbf{x}_t^r$  to

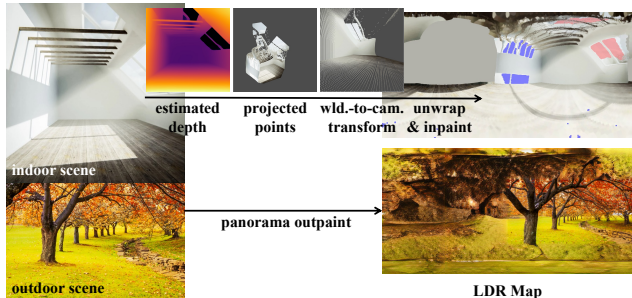


Figure 4. **Pipeline for estimating the LDR map.** We utilize tailored pipelines for indoor and outdoor scenes. Areas masked red and blue correspond to the far light  $\odot$  and near light  $\ominus$  region.

the original  $K$  and  $V$  from  $\mathbf{x}_t$  yielding an image-conditional attention output

$$A(\mathbf{x}_t, \cdot, \mathbf{x}_t^r) = \text{MHSA}(Q, [K; K^r], [V; V^r]), \quad (3)$$

where  $\cdot$  can either be *text* or  $\emptyset$  for text conditioning. In practice, the text-unconditional attention  $A(\mathbf{x}_t, \emptyset, \mathbf{x}_t^r)$  used for classifier-free guidance [23] is reset as  $s_c \cdot A(\mathbf{x}_t, \emptyset, \emptyset) + (1 - s_c) \cdot A(\mathbf{x}_t, \emptyset, \mathbf{x}_t^r)$  weighted by a control guidance scale  $s_c$ . With the percentage  $p$  of blocks to be injected, the intensity of preservation can be controlled:  $s_c = p = 1$  provide the most and  $s_c = p = 0$  the least preservation.

**Blending.** The two components previously mentioned directly utilize object renderings, referred to as the *local view*, as inputs for vanilla SD. To further enhance the adaptation of the object’s appearance to its surroundings, we input the scene image, with the object rendered onto it, referred to as the *global view*, into an additional inpainting SD [49]. We have found that the inpainting model provides superior conditioning on the surrounding environment depicted in the image, resulting in improved blending. However, the inpainting model can sometimes attempt to undesirably modify the inserted object, removing parts of it by inpainting them with the background. To counter this, we compose the *local view* with randomly sample solid background colors, rather than the scene. This prevents the inpainting model from removing parts of the object as the object must look realistic when rendered in front of a random background. In practice, we utilize a set of *global views* created by cropping the original *global view* at various scales, ensuring that the crops encompass the entire *local view*.

### 3.3. Light Estimation

To seamlessly integrate the object into the scene, we estimate the lighting conditions, as outlined in Fig. 4.

#### 3.3.1 Lighting Model

To light the object, we utilize a high dynamic range (HDR) environment map  $\mathcal{E} \in \mathbb{R}^{H_e \times W_e \times 3}$ , which is well-suited for representing natural illumination. Since the given 2D scene

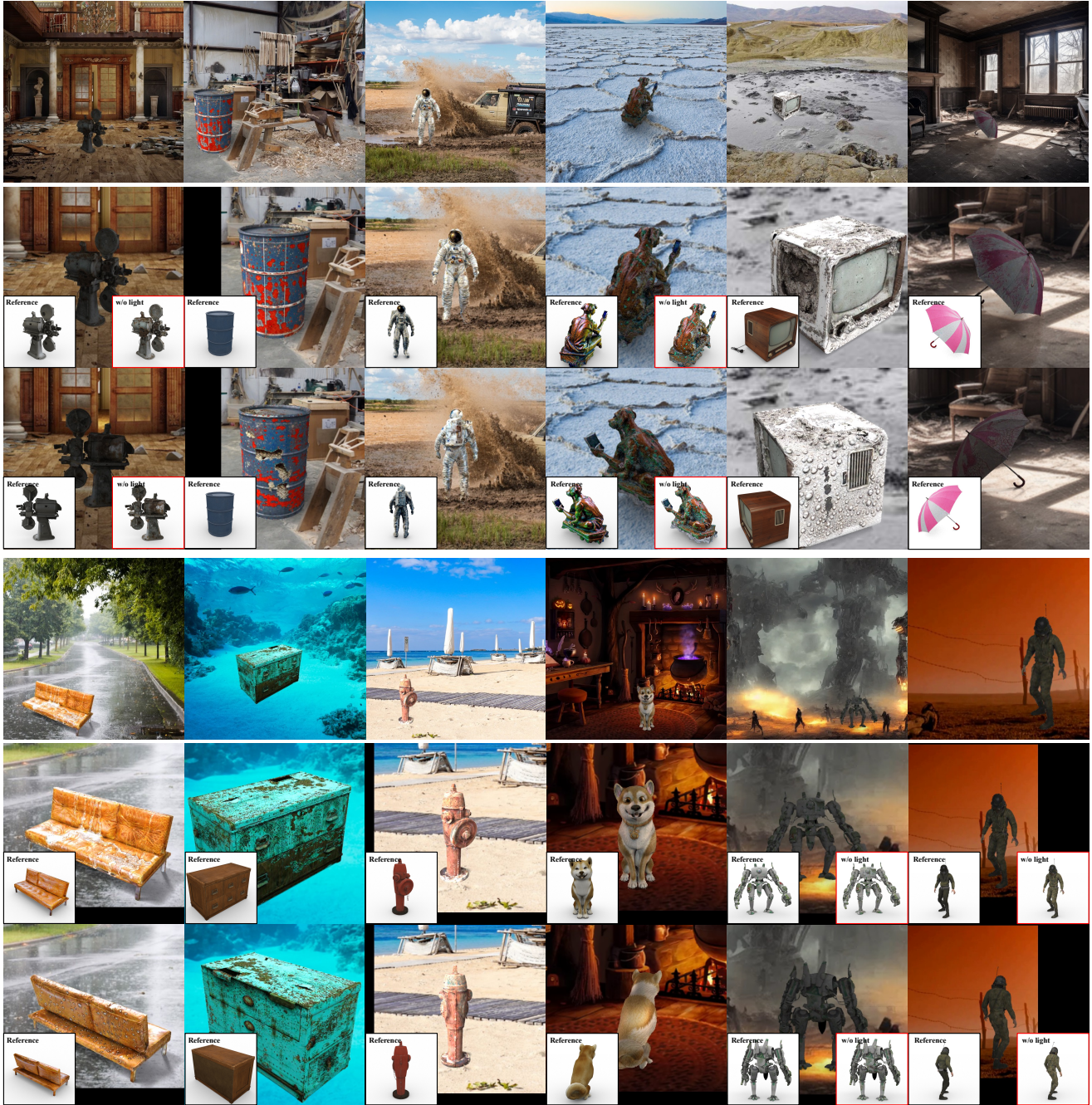


Figure 5. **Visual Results.** We showcase the *global view* (top row) to demonstrate the overall composition quality and object-centric *local view* (bottom two rows) for the fidelity of stylized textures. For dim scenes, we additionally render objects without the estimated lighting condition (*w/o light*) for illustrative purposes.

image only captures a small angle of the full 360-degree environment map, we first use the image as input to estimate a low dynamic range (LDR) environment map. This process depends on the scene type (*i.e.*, indoor vs. outdoor) and is explained in the following paragraphs. Given the LDR map, we then convert it to an HDR map by estimating a light scale (*i.e.*, a scalar) for each bright region, which is thresholded from the LDR map directly (*e.g.*, where intensity  $\mathcal{I}_{i,j} \geq$

0.8). This scalar is then multiplied by the RGB values to approximate an HDR map. Note that we use the HDR map only to light the object, it thus does not need to be of high accuracy to make the object look plausible.

**Indoor Scenes.** The well-bounded 2D visual geometry of indoor scenes is primarily characterized by enclosed spaces and interconnected planes, facilitating straightfor-



Figure 6. **Comparison.** We compare our generated *global view* with the scene-object compositing method: CDC [20] and the *local view* with mesh texturing methods: Prolific Dreamer [59], Fantasia3D [7], and TEXTure [48]. *s.g.d.* denotes similarity guidance. *g.g.d.* and *r.f.i.* denotes global-view guidance and reference feature injection, respectively. Our method achieves both seamless scene-object composition as well as texture adaptation of high fidelity.

ward (rough) 3D reconstruction. To simulate the physical lighting of indoor scenes, we lift each pixel from the 2D scene to 3D space using its estimated depth  $\mathcal{D}$  [13, 47]. We perform world-to-camera and spherical-to-equirectangular coordinate transformations in succession, unwrapping 3D points into a latitude-longitude formatted LDR map. In post-processing, we automatically fill holes and remove small isolated regions. We fill the unseen region (*i.e.* areas behind the camera) with the average RGB value of the 2D scene. Two scalars are optimized: one for the far light region ( $\odot \triangleq \{i, j \mid \mathcal{D}_{i,j} \geq \tau_d \wedge \mathcal{I}_{i,j} \geq \tau_f\}$ ) and another for the near light region ( $\odot \triangleq \{i, j \mid \mathcal{D}_{i,j} < \tau_d \wedge \mathcal{I}_{i,j} \geq \tau_n\}$ ).

**Outdoor Scenes.** 3D reconstruction of outdoor scenes is challenging due to their inherently unbounded geometric structure. Furthermore, in most outdoor scenes, the sun is the dominant light source, and the position change of an object has a negligible effect on the angle shift of the light. Therefore, instead of painstakingly recovering location-specific viewpoints, we opt to use a single-view to panorama outpainting model [2], taking its generated output as the initial LDR map. We optimize one scalar for the far light area with positive elevation ( $\odot \triangleq \{i, j \mid \frac{i}{H_e} < 0.5 \vee \mathcal{I}_{i,j} \geq \tau_o\}$ ), leaving the near light area ( $\odot \triangleq \emptyset$ ) unoptimized. While more sophisticated designs, such as a position estimator [30] or sky modeling [24], could be incorporated, we find our approach robust enough to provide a rough estimation and suggest leaving room for potential enhancements in future work.

### 3.3.2 Light-Capturing Apparatus

To estimate light scales, we place 3D objects with a fixed appearance model into the 2D scene and then we optimize the lighting with VSD as described in Eq. (1) to anchor the lighting impact imposed by the scene. Inspired by the traditional inverse rendering setup [11] where the environment map can almost be perfectly reconstructed from objects’ re-

flections, we introduce a novel concept that incorporates a virtual light-capturing apparatus alongside the object of interest during the optimization process. Specifically, we insert a white sphere made of a smooth diffuse material into the scene, and guide the lighting optimization with the diffusion model using the text prompt “A gigantic diffuse white (spray-painted) sphere (ball)”. The white diffuse sphere proves advantageous in stabilizing lighting estimations for scenes with potentially strong light sources, as the reflected intensity from a white diffuse object closely approximates the intensity of the environmental lighting. In our initial experiments, we also tested spheres with mirrored silver and matte silver materials but found them to be less beneficial.

### 3.3.3 Light-Conditional Guidance

The absence of light conditions in text prompts makes the generated images only loosely constrained on lighting, which is problematic for diffusion models to score the renderings accurately. A white sphere looks gray in a darker environment, so light-agnostic prompts can engender an overestimation of the brightness for dim scenes. Therefore, we append “in a dark environment” if the average intensity of the background and light areas are below certain thresholds. To condition the LoRA-tuned model  $\epsilon_\psi$ , we concatenate the light scales with the camera extrinsic [59] as class embeddings for the U-Net. We find that it helps with more realistic light estimation, especially for outdoor scenes and dimly lit scenes. For scenes with atypical lighting that significantly alters the appearance of objects, we manually append color prompts. For example, we append “in blue tint” for the seabed bathed in blue light, or “in red illumination” for a nightclub enveloped in red atmospheric light.

## 4. Experiments

In this section, we show extensive qualitative results of our method in various settings. Please see the appendix for

many more examples and animations.

### 4.1. Visual Results

We first present visual results and a case study to demonstrate the generalizability of the proposed method. We then compare our method with others that specifically focus on either scene composition or object stylization.

**Main Results.** To demonstrate the generalizability of the framework and the impact of different scenes on the inserted objects, we present visual results in Fig. 5. Our method successfully blends the objects into various environments, achieving photorealistic adaptation for both appearance and lighting. This includes scenarios drawn from both real-world and fantasy settings. For example, the dimly-lit umbrella in Fig. 5 casts a shadow that is perfectly aligned with its handle and the light direction of the scene, substantially increasing the photorealism of the composition; The Belvedere TV set is wrapped with gray mud consistent with the scene while its original structural details get maintained.

**Comparison on Scene Composition.** We showcase the result from CDC [20] using LLM-prompted text prompts for a fair comparison. As shown in Fig. 6, CDC loses the structural details of the object while providing limited adaptation for texture transfer. Moreover, the composed scene appears artificial and synthetic, giving the impression that the sofa is floating above the mud. Our experiments reveal that the CDC often leads to object removal, particularly when the re-painting [34] is employed. Therefore, we further incorporate similarity guidance similar to the classifier guidance [12] by adding  $\sqrt{1 - \alpha_t} \cdot \frac{\partial(\|\mathbf{x}_0^r - \hat{\mathbf{x}}_\phi\|^2)}{\partial \mathbf{x}_t}$  to the predicted gradient  $\epsilon_\phi(\mathbf{x}_t)$  each denoising step referred as **CDC w/ s.g.d.**, but find it provides limited improvement.

**Comparison on Object Stylization.** We showcase results from mesh texturing method [7, 48, 59] using our LLM-prompted text prompts for a fair comparison. As shown in Fig. 6, although achieving realistic texture adaptation, these mesh texturing methods fall short in preserving the original structural details of the object and in utilizing scene-level information. Essentially, These methods only satisfy the *Environmental Influence* requirement via text prompts and do not meet all the criteria of our intended goal.

### 4.2. Ablation Study

**Identity Preservation.** To illustrate how the *Identity Preservation* requirement is satisfied by reference feature injection (*r.f.i.*), we showcase the leather sofa in the swamp with less and more control (Fig. 7). The setup with less control drifts to a visually different sofa with too much mud wrapped around while more control generates a less muddy and adapted sofa compared to the reference image. Both adapted textures are less visually plausible. Additionally, when comparing **Ours w/o g.g.d. & r.f.i.** to the reference



Figure 7. **Ablation on Texture Adaptation.** We ablate global-view guidance (*g.g.d.*) and reference feature injection (*r.f.i.*). *-ctrl.* and *+ctrl.* denotes less or more control in feature injection (smaller or higher  $s_f$  &  $p$ ) for *Identity Preservation* requirement.

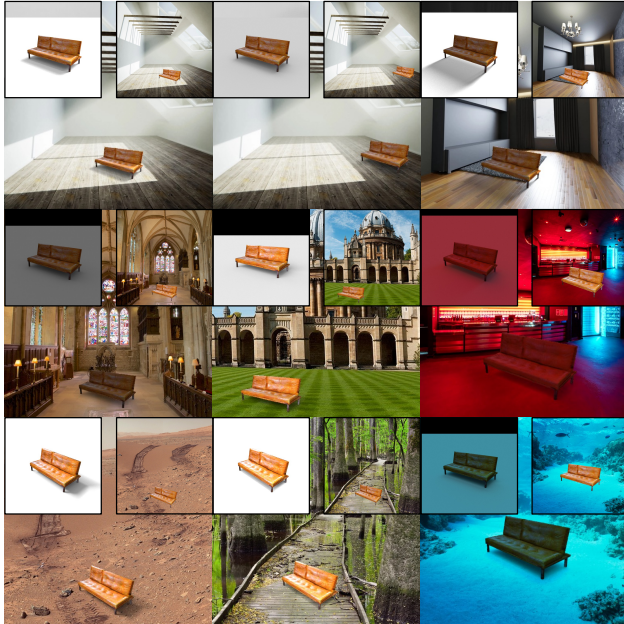


Figure 8. **Ablation on Light Estimation.** We evaluate the effectiveness of light estimation by demonstrating the lighting effects on a sofa in various indoor and outdoor scenes.

image, it is evident that the identity of the sofa is lost.

**Global-View Guidance.** To showcase the necessity of global-view guidance we conduct texture adaptation without it as **Ours w/o g.g.d.** in Fig. 7. The adapted texture without seeing the full scene fails to adapt the color of the mud to that of the scene image, contrasting starkly with the scene. Experiments ablating the optimal global-view guidance set-up (*e.g.*, solid-color background augmentation, usage of inpainting model, *etc.*) are detailed in the appendix.

**Light Estimation.** In Fig. 1, the combination of accurately estimated lighting and shadows significantly enhances the photorealism of the composed image (compare the image on the left, which includes lighting, to those in the top right corner, which are without lighting). To further test the validity of the estimated light, we render images omitting the texture adaptation step. Fig. 8 demonstrates that the estimated light considers multiple factors, including its direction relative to the specific locations of objects in indoor scenes and its impact on the appearance of objects under atmospheric colored lighting conditions. Importantly, the estimated HDR maps, paired with the proposed scene composition, facilitate the realistic integration of shadows.

## 5. Conclusion

In this paper, we are motivated by a practical goal—*what if a 3D object is placed into a 2D scene?*—and propose a novel framework that allows (1) stylizing the object with an adapted texture that aligns with the given scene; and (2) achieving a photorealistic scene composition with the aid of estimated light of the environment. This is enabled by physically-based differentiable ray tracing and diffusion models used as guidance. Our method allows for automatic adaptation and blending of existing objects into a variety of scenes, making it useful for both 2D and 3D downstream applications, such as media production and video games.

**Acknowledgement.** This work is supported by the UKRI grant: Turing AI Fellowship EP/W002981/1 and EP-SRC/MURI grant: EP/N019474/1. J. Z. is also supported by the Horizon Robotics. We thank Luke Melas-Kyriazi and Fabio Pizzati for helpful discussions.

## A. Additional Visual Results

Additionally, we conduct a case study in Fig. 9, where we specifically place a sofa into a diverse array of scenes. For the last two cases in Fig. 5 (*robot* and *human avatar*), we first conduct textual inversion [14] for local-view guidance and find it slightly better than using vanilla SD in keeping the object’s identity and structural details. We find that the method can deal with a wide variety of objects and environments.

We encourage readers to check out our project page for many more visual results, animated results, and videos demonstrating the training dynamics.

## B. Additional Ablation Study

### B.1. Texture Adaptation: Meta Setup

In this section, we conduct ablative studies on the meta-setup for texture adaptation *without applying the estimated light*. Summarized as in Tab. 2, we first study the effectiveness of GPT prompts ((d) – (e)) and compare the proposed reference feature injection with employing InstructPix2Pix [3] as guidance ((f) – (h)) similar to *scene-agnostic* setup detailed in Appendix C.1 with differences on the choice of the model and prompts. Further, studies investigating the optimal setup of how to incorporate global-view guidance ((i) – (o)) are conducted.

**Manual vs. GPT-Prompted Text Prompts.** We ablate the necessity of GPT-prompted text prompts by comparing (d) to (e) and (f) to (g) in Tab. 2. Compared with the manually designed prompts, the GPT-prompted ones lead to more expressive and versatile textures, vividly showcasing the potential *Environmental Influences* the scene can exert on the objects.

**Reference Feature Injection vs. InstructPix2Pix [3]** We compare the capability balancing transfer and control with InstructPix2Pix [3], validating the effectiveness of the proposed reference feature injection module. Comparing (g) to (h), InstructPix2Pix drastically shifts the structural details and identity of the original sofa. The adapted texture from InstructPix2Pix also appears to be less realistic.

**Vanilla vs. Inpainting Model.** Two factors can be considered when incorporating scene-level guidance: the scene-conditional text prompts and the scene-conditional background. We find that it is better to bind the scene-composed image with an inpainting SD to account for the *Blending* requirement. Comparing (l) to (m), the inpainting SD encourages the generated textures to be more related to the scene content. We observe that it is crucial to use GPT-prompted prompts for the vanilla SD. Comparing (k) to (o), not using GPT-prompted prompts leads to a much more expressive and adapted texture.

**Scene vs. Solid-Color Background Composition.** The input to vanilla SD is object renderings composed with a solid background to ensure objects not camouflaging into the scenes. Comparing (n) to (o), a solid background helps to enhance the clarity of the object’s boundary pixels. In (i) where only vanilla SD is used for scene-composed input, the legs of the sofa are entirely blended into the muddy ground, rendering it unrecognizable and inappropriate for downstream usage.

### B.2. Light Estimation

In this section, we conduct ablation studies on setup for light estimation, justifying the usage of the light-conditional guidance and light-capturing apparatus in stabilizing the estimation.

**Light Capturing Apparatus.** We ablate the necessity of a diffuse ball. As shown in the first two rows of Fig. 11, adding a white diffuse sphere helps to locate the dominant light and optimize its range into a reasonable range.

**Light-Conditional Guidance.** As mentioned before, adding the dark prompt and color prompt helps optimize for dark scenes and scenes with atypical lighting. As shown in the last two rows of Fig. 11, light estimation without light-conditional guidance appears to be too bright for the *seabed*.

### B.3. Composition

We ablate in this section whether to apply the estimated light condition during the texture adaptation step or only use it in the final rendering for scene composition. We observe that the integration of an HDR map in the texture adaptation step yields less versatility in the generated texture. Nonetheless, in scenarios where the lighting is atypical, such as poorly lit scenes or environments bathed in colored illumination, it is necessary to utilize the HDR map to ensure that the environmental lighting does not unduly influence the appearance of objects.

**Texture Adaptation without HDR Map.** As shown in Fig. 12, applying the estimated HDR map during texture adaptation leads to comparatively less expressive adaptation and visual transfer. If the object is poorly lit as the input to the diffusion model, it is hard for the model to derive a clear denoised supervisory signal.

**Texture Adaptation with HDR Map in Atypical Lighting.** As shown in Fig. 13, omitting the estimated HDR map results in the unintended spill of lighting effects into the object’s appearance. Applying the HDR map at the post-texturing stage adversely impacts the photorealism, contracting the optimized texture.

## C. Scene-Agnostic Texture Generation

Without tailored design incorporating 2D scenes for mesh texturing, our pipeline effectively serves as a perfor-



Figure 9. **Case Study.** We showcase the *global view* (top row) to demonstrate the overall composition quality and object-centric *local view* (bottom two rows) for the fidelity of stylized textures for a wide range of different scenes using the same original object: a leather sofa.

	Global-View Guidance			Local-View Guidance		
	Background	Model	Prompt	Background	Model	Prompt
<i>Scene-Agnostic</i>						
(a)	-	-	-	solid color	vanilla SD	object
(b)	-	-	-	solid color	InstructPix2Pix [3]	manually instructed*
(c)	-	-	-	solid color	vanilla SD w/ <i>r.f.i.</i>	manually combined*
<b>+ Environmental Influence</b>						
(d)	-	-	-	solid color	vanilla SD	manually combined
(e)	-	-	-	solid color	vanilla SD	GPT-prompted
<b>+ Environmental Influence + Identity Preservation</b>						
(f)	-	-	-	solid color	InstructPix2Pix [3]	manually instructed
(g)	-	-	-	solid color	InstructPix2Pix [3]	GPT-prompted
(h)	-	-	-	solid color	vanilla SD w/ <i>r.f.i.</i>	GPT-prompted
<b>+ Environmental Influence + Identity Preservation + Blending</b>						
(i)	-	-	-	scene	vanilla SD w/ <i>r.f.i.</i>	GPT-prompted
(j)	scene	vanilla SD	manully combined	solid color	vanilla SD w/ <i>r.f.i.</i>	object
(k)	scene	vanilla SD	GPT-prompted	solid color	vanilla SD w/ <i>r.f.i.</i>	object
(l)	scene	vanilla SD	GPT-prompted	scene	vanilla SD w/ <i>r.f.i.</i>	object
(m)	scene	inpainting SD	GPT-prompted	scene	vanilla SD w/ <i>r.f.i.</i>	object
(n)	scene	inpainting SD	GPT-prompted	scene	vanilla SD w/ <i>r.f.i.</i>	GPT-prompted
(o)	scene	inpainting SD	GPT-prompted	solid color	vanilla SD w/ <i>r.f.i.</i>	GPT-prompted

Table 2. **Ablative Study on Meta Setup for Texture Adaptation.** (a) is *scene-agnostic texture generation* setup as described in Appendix C.1. (c) is *scene-agnostic texture editing* setup as described in Appendix D.1. (o) is the complete *scene-conditional texture adaptation* setup as described in Appendix E. \* denotes for scene-agnostic text prompts considering the given instruction. For example, with the object prompt being *a leather sofa*, the manually instructed prompt can be “*add the dusting to the sofa*” and the manually combined prompt can be “*a leather sofa with dust*”.

mant baseline on texturing textless meshes. We first detail its set-up in Appendix C.1, summarized as (a) in Tab. 2, and further compare it with the latest state-of-the-art methodologies [4, 6, 7, 48, 59] in Appendix C.2.

## C.1. Implementation Details

**Camera and Light Sampling.** We sample over 72 views uniformly across azimuth  $a \in [0^\circ, 360^\circ]$  and elevation

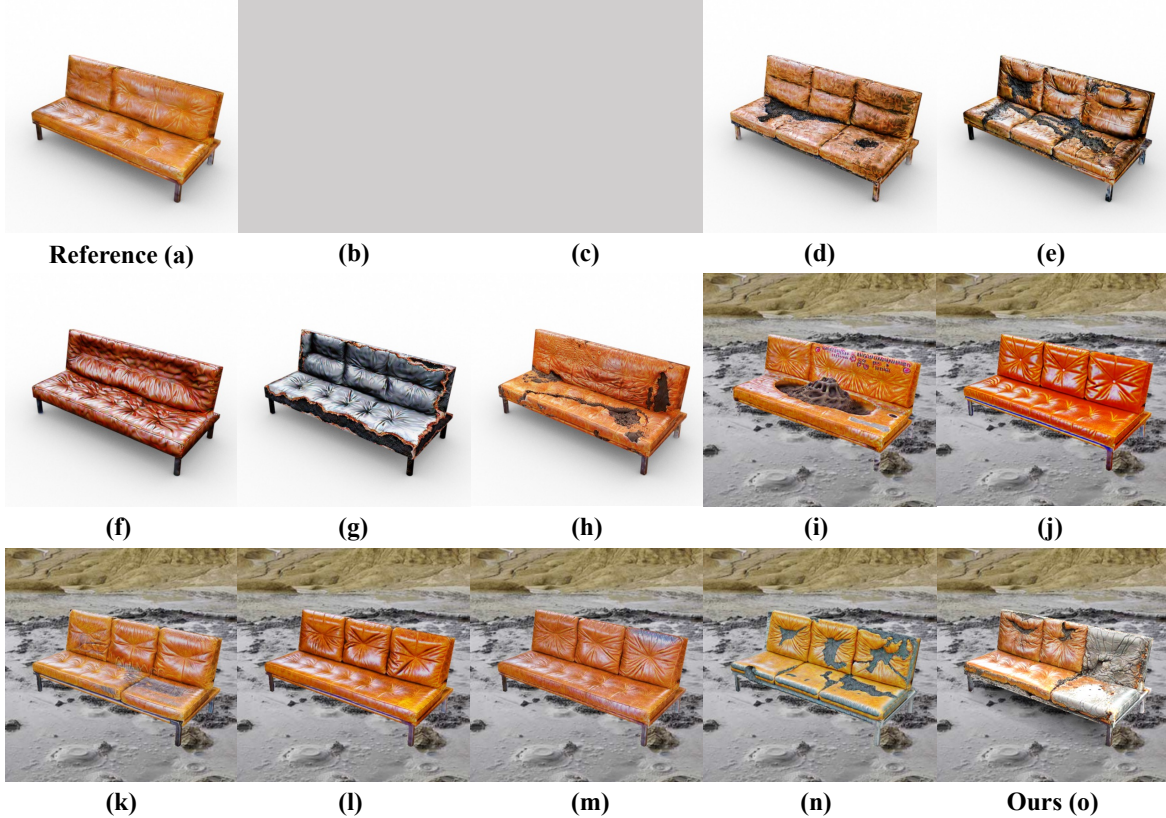


Figure 10. **Additional Ablation on Texture Adaptation.** We study the impact of different modules on adapted textures. (d) and (e) utilized scene-conditional text prompts to meet the *Environmental Influence* requirement. (f) – (h) studies how *Identity Preservation* can be better achieved. (i) – (o) studies how to leverage scene background during adaptation, aiming for desirable *Blending* with objects’ placed context.

$e \in \{20^\circ, 30^\circ, 45^\circ\}$  with small perturbations. We observe that entirely random sampling in Mitsuba3 [26] leads to unknown memory leakage issues and rendering speed downgrade. We leave this for future fixes since it may require dedicated optimization of its compiler [27] from Mitsuba3’s team. Differently, we sample  $\lambda_{\text{FOV}} \in [0.6, 1.21]$  to include detailed close-up renderings of object parts, enhancing generation fidelity. For light sampling, we use ambient lighting with the light scale being all 1.0 by default and sample environment maps with one dominant light source by a probability  $p$ . Specifically, we model the light as an isotropic spherical Gaussian following [16], parameterized by  $c_x \in [0, 1.0]$ ,  $c_y \in [0, 0.5]$ ,  $c_r = 0.08$ , and  $c_v \in [12.0, 15.0]$ , denoting the x-coordinate of the Gaussian’s center, y-coordinate of the Gaussian’s center, radius, and its intensity. The background is simply parameterized by  $b_v = 0.8$  as its intensity. See coordinate conventions<sup>1</sup> for the environment map used in Mitsuba3 for details. In practice, enabling environment map augmentation with a positive  $p$  helps to alleviate the shortcut learning of reflectance as diffuse texture for highly reflective surfaces.

<sup>1</sup>[https://mitsuba.readthedocs.io/en/latest/src/generated/plugins\\_emitters.html#is2](https://mitsuba.readthedocs.io/en/latest/src/generated/plugins_emitters.html#is2)

**Solid Color Composition.** We compose the object in the background with a default solid color  $[0.5, 0.5, 0.5]$  and augment it with a probability  $p = 0.5$  with random solid colors. Alternatively, learning a background prediction network conditioned on camera poses is testified to be of little help. We discard the rendered shadow when composing it with the object rendering.

**Textless Mesh.** We consider two main sources of textless meshes: (1) mesh generated from scratch [7, 59] with text prompts and SD guidance in Deep Marching Tetrahedra [51] (DMTet); and (2) mesh downloaded from online assets [1, 10].

**Model, Prompt, and Guidance.** We use vanilla SD (stabilityai/stable-diffusion-2-base) as the guidance diffusion model with a classifier-free guidance [23] of 7.5. A  $\lambda_t \in [0.9, 1.0]$  is used to compare with other methodologies in Appendix C.2. However, we find that VSD tends to overfit 3D objects in a specific condition, such as lighting, leading to excessive noises and unnecessary details. Hence, it is sometimes essential to opt for an even smaller  $\lambda_t$  (i.e., 0.6) when *scene-agnostic texture generation* setup is used as an initial stage for the texture adaptation step

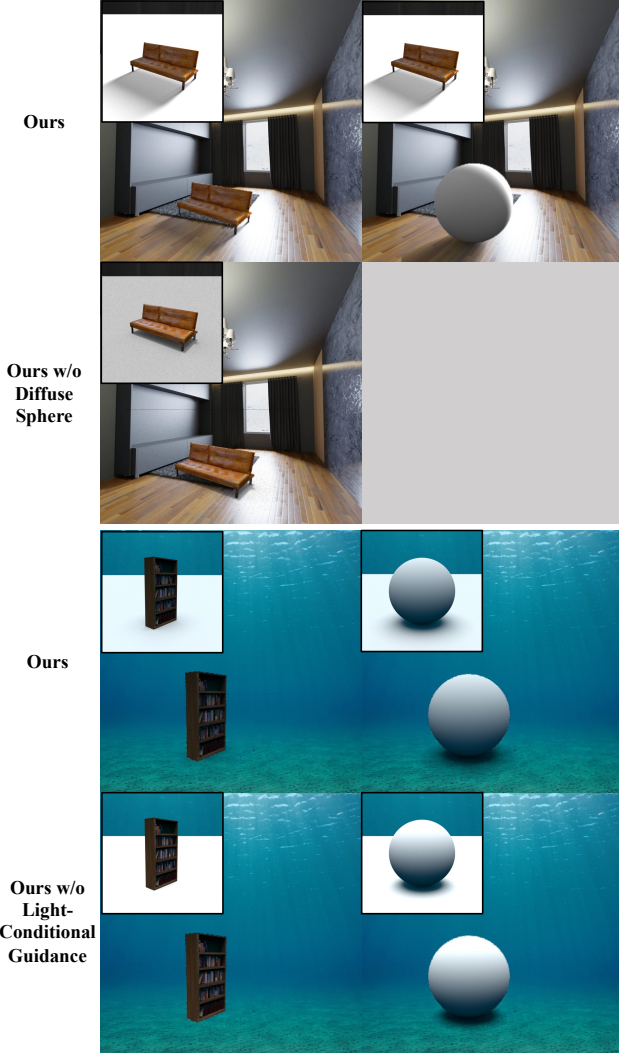


Figure 11. **Additional Ablation on Light Estimation.** **Ours** denotes the complete setup. We ablate the necessity of light-conditional guidance (first row *vs.* second row) and the white diffusive sphere (third row *vs.* last row). Without the diffuse sphere (top) the intensity of the dominant light source from the window is undesirably estimated. Without the light-conditional guidance (bottom), the objects appear to be overly bright and do not fit in the dark blue atmosphere of the seabed.

followed, leaving room to cultivate scene-conditional details, especially for simpler objects. We use object prompts with view-dependent prompting as in [43, 59] but without light-dependent prompting, since we only sample properly-lit light conditions. Notably, we condition the LoRA-tuned model  $\epsilon_{\psi}$  not only on light scales  $c_v$  and  $b_v$  but also on  $c_x$ ,  $c_y$ , and  $c_r$  as a 5-dimensional vector. For default ambient lighting, we set  $c_x = 0.25$  (*i.e.*,  $0^\circ$  azimuth),  $c_y = 0$  (*i.e.*,  $90^\circ$  elevation),  $c_r = 0$ ,  $c_v = 1.0$ , and  $b_v = 1.0$ .

**Stage-Wise Optimization.** By employing a coarse-to-fine 2-stage optimization, the pipeline strikes a balance be-

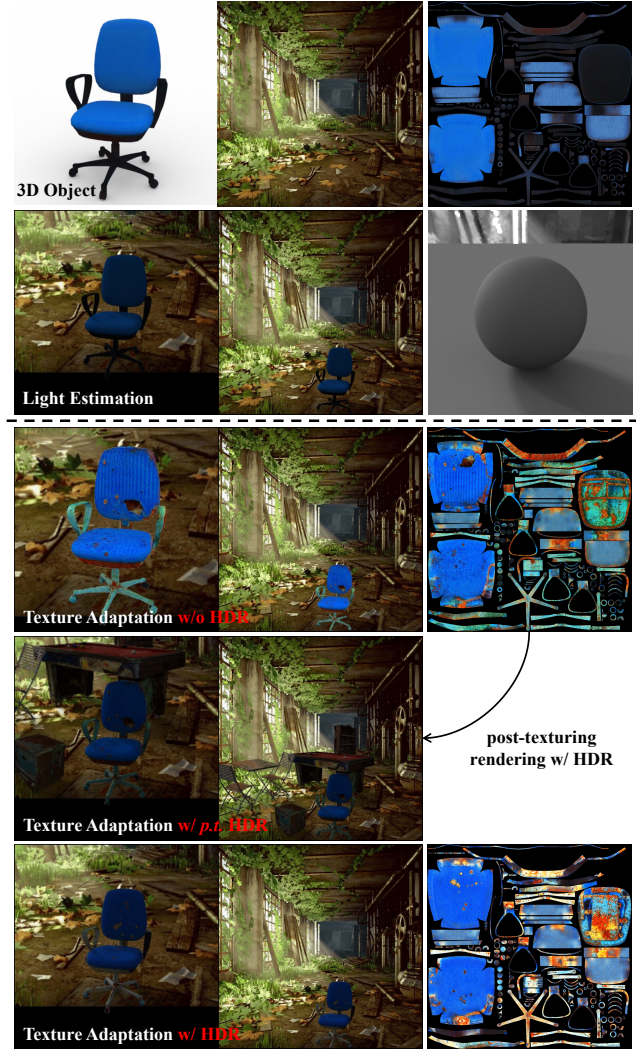


Figure 12. **Texture Adaptation without HDR map.** During texture adaptation, we use default ambient light during texture adaptation (w/o HDR, third row) and further apply the estimated HDR map at the post-texturing (*p.t.*) rendering stage (w/ *p.t.* HDR, fourth row). Alternatively, one can initialize the HDR map (w/ HDR, last row) optimized from the light estimation stage (second row) to decouple potential environmental lighting effects from appearance effects. The text prompt we use is “*The wheeled office chair, upholstery gone, structure rusted, wheels seized, enmeshed in vegetation, forgotten relic of a bygone era.*”

tween between performance and efficiency. For the first coarse stage, we use a rendering resolution of 256 (and further resized to 512) and samples per pixel of 64. Noises  $\epsilon$  with  $t \in [30, 990]$  are sampled, ensuring a sufficient level of diversity. For the second fine stage, we use a rendering resolution of 512 and samples per pixel of 128. Noises  $\epsilon$  with  $t \in [500, 990]$  are sampled. A total of 4000 iterations are conducted with training distributed across 4 GPUs. Two stages are split with a ratio of [0.2, 0.8]. A constant learning rate of 0.001 for the texture MLP and 0.0001 for LoRA-

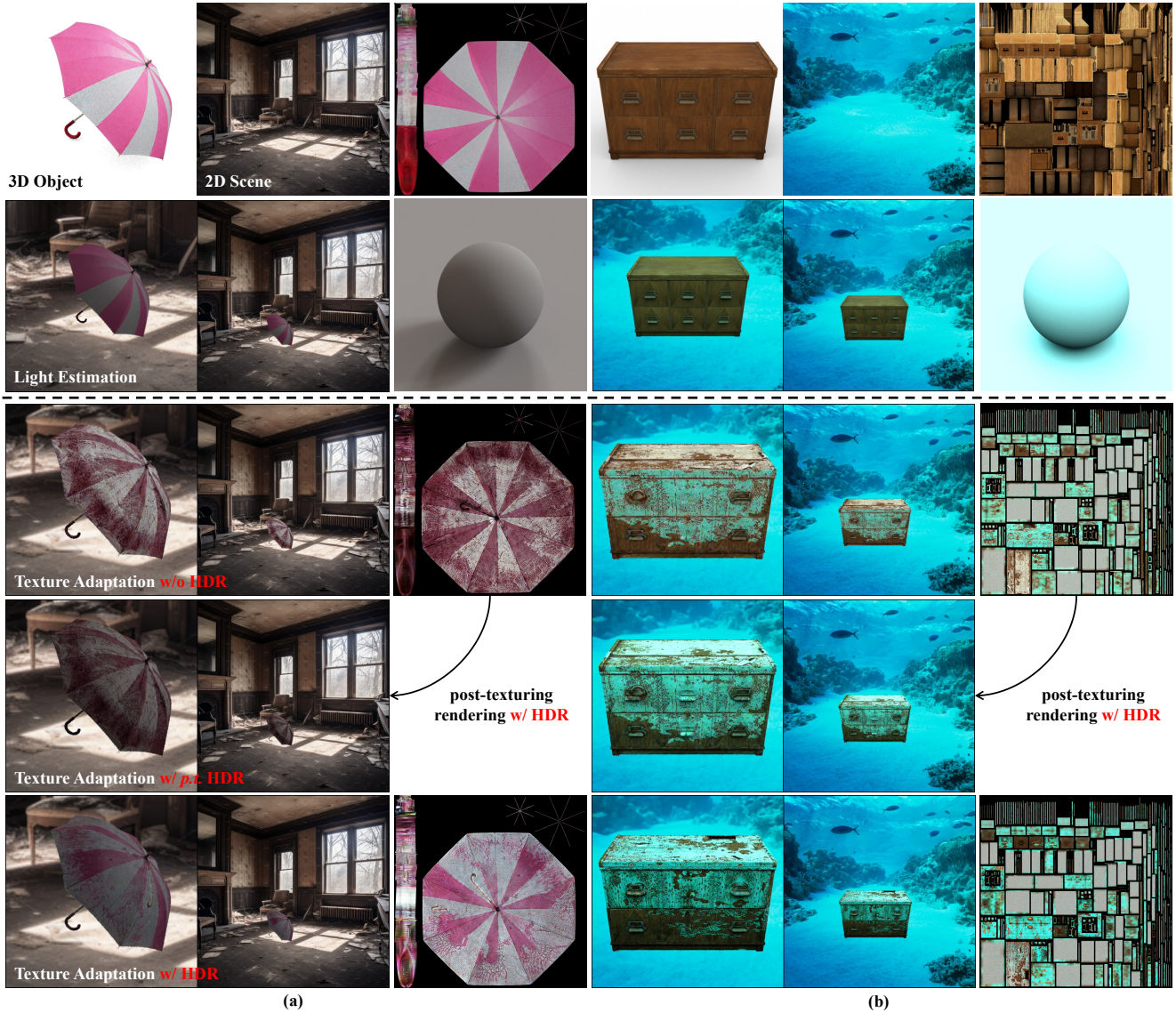


Figure 13. **Texture Adaptation with HDR map in atypical lighting.** During texture adaptation in atypical lighting, we initialize the HDR map (w/ HDR, last row) optimized from the light estimation stage (second row) to decouple potential environmental lighting effects from appearance effects. Alternatively, one can use default ambient light during texture adaptation (w/o HDR, third row) and further apply the estimated HDR map at the post-texturing (*p.t.*) rendering stage (w/ *p.t.* HDR, fourth row). Two cases are considered with text prompts (a) “Umbrella, dusty, partly opened, shadowed, cobwebs draping, amidst decaying furniture;” and (b) “Vintage wooden drawer, swollen, colors faded, surfaces colonized by marine life, partly buried in sandy ocean floor, corroding metal fixtures.”

tuning parameters are applied.

## C.2. Visual Comparison

Comparison with two groups of methods: one based on *texture wrapping* [6, 48] and the other based on *score distillation* [7, 59] are conducted. Although the boundary between two categories is obscure given formulation in Eq. (2) and the gap can be bridged [19, 62], we stick to the taxonomy to incorporate all existing methods for a comprehensive comparison.

sive comparison.

In Fig. 14, our method demonstrates superior photo-realistic texture generation, leveraging VSD. Our results align closely with those of ProlificDreamer [59], surpassing the comparatively cartoonish and saturated textures produced by Fantasia3D [7]. We note that it is imperative to use a small  $\lambda$  for objects with simple textures (*e.g.*, the *umbrella*). Compared to ProlificDreamer which yields over-texturized texture, our method achieves reasonable texture

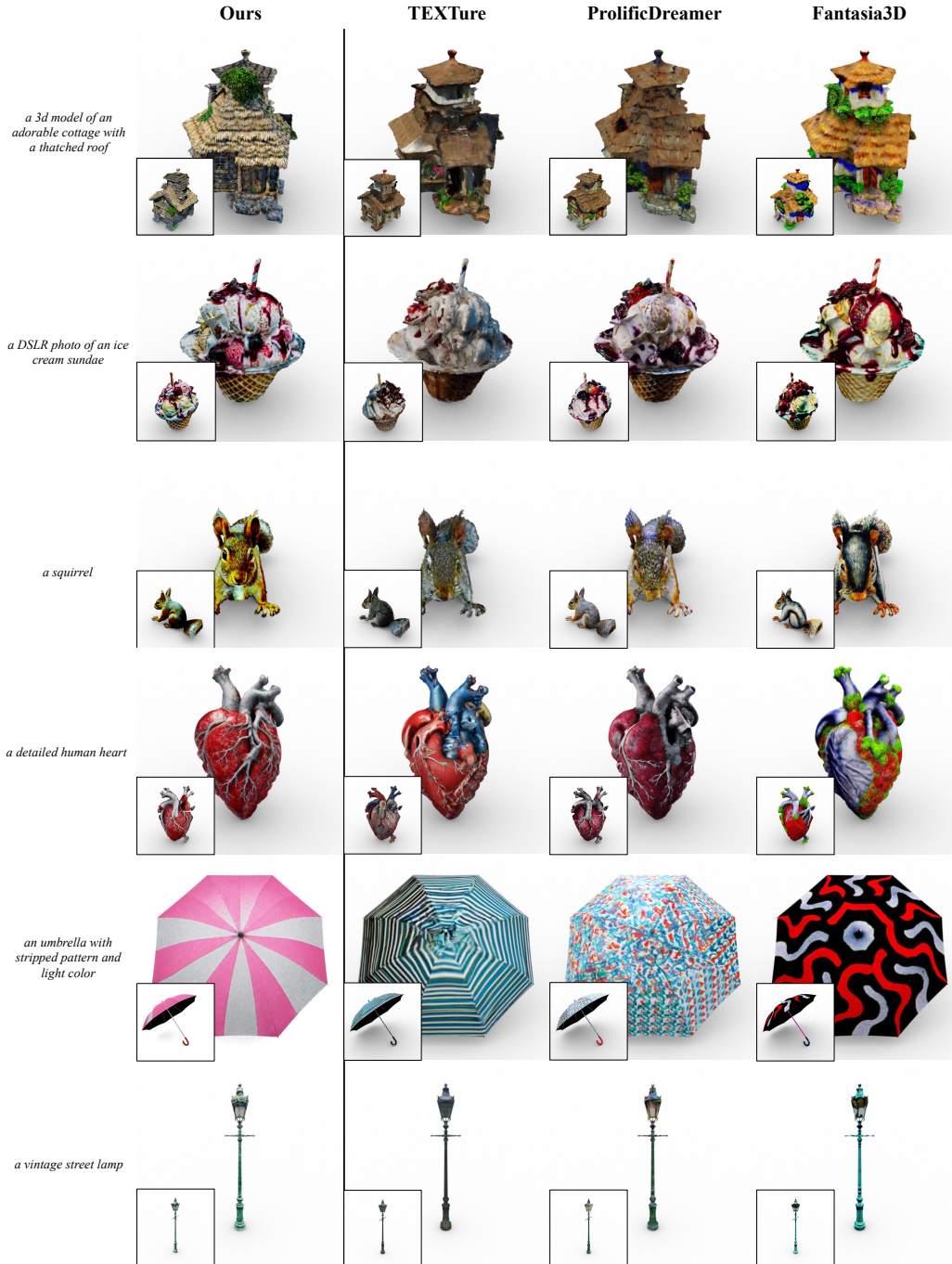


Figure 14. **Scene-Agnostic Texture Generation.** We compare our framework with mesh texturing methods: Prolific Dreamer [59], Fantasia3D [7], and TEXTure [48]. We consider textless meshes generated from text prompts or downloaded online.

for the *umbrella*. Compared to TEXTure [48] which generally lacks consistency over multiple views (*e.g.*, the *heart*), methods based on *score distillation* provide a more cohesive and believable appearance.

## D. Scene-Agnostic Texture Editing

### D.1. Implementation Details

We follow the setup for **camera and light sampling** and **solid color composition** as in Appendix C.1. Since we are editing a textured mesh, we follow **textured mesh with**

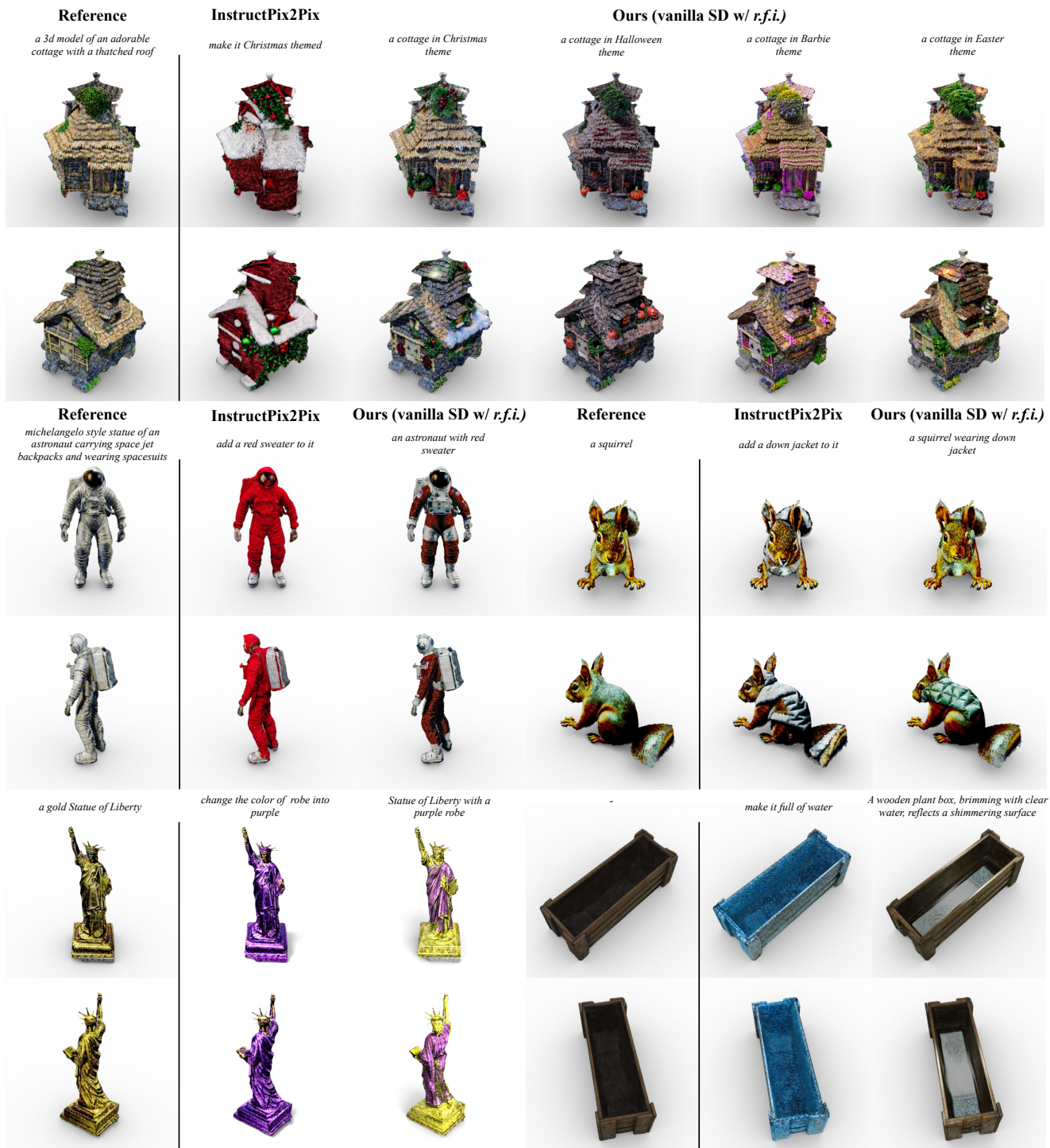


Figure 15. **Scene-Agnostic Texture Editing.** We compare our framework with InstructPix2Pix [3] by replacing vanilla SD with reference feature injection (*r.f.i.*). We use textured meshes generated from text prompts or from existing downloaded textures as input.

**neural texture** as in Appendix E to start from an initialized MLP weight, mitigating potential content drift. We use the vanilla SD (stabilityai/stable-diffusion-2-base)

with reference feature injection as the guidance diffusion model with a classifier-free guidance [23] of 7.5. We use a  $\lambda_t = 1.0$ . We manually combine the object prompt (e.g., *the*

leather sofa) and the instruction (e.g., *add sofa with dust*), yielding one describing the edited object’s appearance (e.g., *a leather sofa with dust*). Noises  $\epsilon$  with  $t \in [500, 990]$  are sampled with a rendering resolution of 512 and samples per pixel of 128. A total of 4000 iterations are conducted with training distributed across 4 GPUs. The setup is summarized as (c) in Tab. 2.

## D.2. Visual Comparison

We evaluate using InstructPix2Pix [3] as the guidance model and the instruction as text prompts, summarized as (b) in Tab. 2. Compared to InstructPix2Pix, vanilla SD with *r.f.i.* achieves more fine-grained and accurate visual control. For example, while InstructPix2Pix successfully transforms the *cottage* into a Christmas theme, it erases the object’s original identity. Ours (vanilla SD with *r.f.i.*) adds elements to the original *cottage* (e.g., *snow on the roof* and *mistletoe at the top*), achieving a well-balanced integration of visual transfer and control.

## E. Implementation Details

**Camera Sampling.** We sample 24 views with an azimuth uniformly sampled across  $360^\circ$  and a user-specified elevation  $e$ . We sample a FOV multiplier  $\lambda_{\text{FOV}}$  such that camera FOV is  $\tanh(\frac{r \cdot \lambda_{\text{FOV}}}{d_{\text{cam}}})$  where  $r = 0.5$  is the maximal range of normalized vertices and  $d_{\text{cam}} = 2.0$  is the camera distance. A rendering resolution of 512 and samples per pixel of 128 are used during training, while samples per pixel of 1024 are used for evaluation.

**Scene Composition.** To insert the object into the scene image, we directly alpha-blend the 2D rendering of the object with the scene image according to the user-provided position and size. To allow for object shadows, we model an infinitely expansive floor as a plane where the 3D object is placed. Isolating the shadow from its white background can be done by simple thresholding based on the average intensity of the rendered floor, resulting in two regions: shadowed region  $R_s$  and lit region  $R_l$ . We scale the intensity of pixels in  $R_s$  with a scalar  $\frac{\text{norm}([1, 1, 1])}{\mathbb{E}(\{I_{i,j} \mid i,j \in R_l\})}$  and further convert the scaled intensity into transparency.

**Textured Mesh with Neural Texture.** We consider two sources for the textured mesh with its neural texture, with which the MLP weights of the appearance model can be initialized:

- For meshes textured with text prompts and SD guidance, we directly resume the MLP weights. See Appendix C for its implementation details and a comparison with other scene-agnostic texturing methods.
- For meshes downloaded online that come with an existing texture, we first convert them into the neural texture by optimizing the neural network’s parameters us-

ing inverse rendering to match the original texture, using a learning rate of 0.02 annealed to 0.001 for a total of 1000 iterations on 1 GPU.

We bake the texture map and re-map the UVs if multiple materials exist. We re-mesh the mesh and interpolate the UVs if there are large faces.

**Texture Adaptation.** For PBR shading model in Mitsuba3 [26] API, we opt for the principled BSDF with  $k_d$  as base\_color,  $k_r \in \mathbb{R}^1$  as roughness, and  $k_m \in \mathbb{R}^1$  as metallic. We sample  $\lambda_{\text{FOV}} \in [1.0, 1.21]$ , avoiding degeneration on fidelity due to rendering resolution. We use a fixed ambient light.

As summarized in Tab. 2, we use (m) as the complete setup. Specifically, we use a vanilla SD (stabilityai/stable-diffusion-2-base) for local-view guidance with *local view* (i.e., the object rendering composed with solid color) as input and an inpainting SD (stabilityai/stable-diffusion-2-inpainting) for global-view guidance with scene-composed *global views* as input. The local-view and global-view guidance contribute equally to the final loss. A  $\lambda = 1.0$ , a control guidance  $s_c = 0.0$ , a percentage of  $p = 1.0$  for feature injection, a classifier-free guidance [23]  $s_{cf} = 7.5$ , and noise levels with  $t \in [500, 990]$  are used by default. We find that annealing noise levels from high to low is beneficial in achieving textures of less noise, particularly when utilizing reference feature injection. We train the MLP with a constant learning rate of 0.001 and LoRA weights for  $\epsilon_\psi$  with a constant learning rate of 0.0001 for a total of 4000 iterations. The optimization is distributed over 4 GPUs with each sampling one view of the object.

To meet the *Identity Preservation* requirement, one could also use InstructPix2Pix [3] (timbrooks/instruct-pix2pix) as in [21, 29] alternatively. We ablate such an option in Appendix B.1 and find that InstructPix2Pix significantly limits versatility and generation quality, due to information loss incurred during their fine-tuning stage on a constrained instruction dataset. Additionally, we also consider a *scene-agnostic texture editing* setup in Appendix D by converting the instructions into appearance descriptions. The experiments reveal that our method is a performant alternative for general instruction-following 3D editing tasks, providing much more fine-grained and accurate control.

**Light Estimation.** For post-processing for indoor scenes, we use `cv2.inpaint()` to fill holes and `cv2.morphologyEx()` to remove small isolated regions. To locate the bright areas, we use  $\tau_f = 0.8$ ,  $\tau_f = 0.95$ ,  $\tau_o = 0.9$ , and  $\tau_d = +\text{inf}$ . We set  $\lambda_{\text{FOV}} = 1.65$  to include the potential full shadow.

We use two *global views* only as input for vanilla SD (stabilityai/stable-diffusion-2-base): one always containing the full scene and one interpolated by cropping the

full scene. For light-dependent prompting, if the average intensity of the background areas  $\mathbb{E}(\{\mathcal{I}_{i,j} \mid i, j \notin \odot \wedge i, j \notin \heartsuit\}) < 0.2$  and the average intensity of light areas  $\mathbb{E}(\{\mathcal{I}_{i,j} \mid i, j \in \odot \vee i, j \in \heartsuit\}) < 50.0$ , we append “in a dark environment”. Two viewpoints are forwarded to vanilla SD and supervised by VSD with the object prompt (with light-dependent prompting but without view-dependent prompting), a  $\lambda = 1.0$ , a classifier-free guidance [23]  $s_{cf} = 7.5$ , and noise levels with  $t \in [750, 990]$ . We train the light scales with a learning rate of 0.01 and LoRA weights for  $\epsilon_\psi$  with a learning rate of 0.0001, all linearly annealed to  $0.1\times$  through a total of 2000 iterations. The optimization is distributed over 4 GPUs, with 3 each sampling one view of the object and the other sampling the sphere. We rescale the loss from each GPU with ratios  $\{\frac{1}{6}, \frac{1}{6}, \frac{1}{6}, \frac{1}{2}\}$  to balance the contributions from the object and the sphere.

By default, the light estimation step is performed separately from the style adaptation step only to enhance the photorealism of the composition. One can perform light estimation first and reuse the estimated light during texture adaptation to disentangle potential lighting effects from being baked into textures. Our observation reveals that this yields less versatile texture especially when object parts are in shadow or strongly lit. However, for atypical lighting conditions such as dimly-lit scenes or environments with colored light, applying the estimated HDR maps during texture adaptation helps prevent the lighting effects from being baked into the texture map. Refer to Appendix B.3 for a detailed ablation study.

## F. Prompting with GPT-4

We detail the prompt used for prompting GPT-4 in Tab. 3. The generated prompts are denoted as *GPT-prompted* in Tab. 2 as opposed to the *manually combined* ones (e.g., *a leather sofa in a swamp*). We encourage GPT-4 to prioritize examining physical effects while leaving the consideration of lighting to the light estimation step. The follow-up instructions can be given from the users to provide more tailored details. We encourage the user to first generate some 2D images using the text prompts to check if the output meets expectations.

**Prompting for InstructPix2Pix [3].** Similarly, to automatically generate scene-conditional text prompts for InstructPix2Pix to involve the *Environmental Influence*, we use LLM to prompt for InstructPix2Pix, as studied in Appendix B.1. As detailed in Tab. 4, we prompt GPT-4 to give instructions instead of appearance descriptions for the final step after the analysis. The generated prompts are denoted as *GPT-prompted* in Tab. 2 as opposed to the *manually instructed* ones (e.g., “place the leather sofa in the swamp”).

---

### Prompting GPT-4 with optional visual input

---

User	<p>[the scene]: the given image (or <i>a chaotic painting studio</i>)          [the object]: <i>a leather sofa</i></p> <p>Now, imagine a picture where [the object] is placed into [the scene]. First, detailedly discuss the environmental impacts of [the scene] imposes on the appearance of [the object]. Focus on the physical impacts instead of lighting impacts.</p> <p>Then provide a succinct, purely descriptive, short, and mechanistic description of the appearance of [the object] inside [the scene] concatenated with “;”. Aim the description to be approximately 25 to 35 words in length. Use simple language. Include all words provided in [the object].</p>
User (optional)	
GPT-4	<p>In the given scene, which is a spacious and sunlit artist’s studio cluttered with art supplies, canvases, and paint splatters, a leather sofa would become part of the creative tableau. The sofa would likely gather paint stains, dust, and perhaps even impressions from various tools and materials used in the studio. The natural lighting from the large windows could cause the leather to fade over time, especially if it’s exposed to direct sunlight.</p> <p>The mechanistic description of the leather sofa in this scene would be: “<i>A leather sofa, stained with streaks and specks of paint, nestles amidst scattered canvases and brushes, its surface a testament to the studio’s artistic endeavors.</i>”</p>
User	Let’s suppose the leather sofa has been placed in the painting studio for decades. Consider the consequences and give me another description.
GPT-4	<i>A leather sofa, surface cracked and color faded, sits under a veil of dust and dried paint splatters, a silent witness to the studio’s years of creative toil.</i>
User	Let’s suppose the leather sofa has just been placed. Consider the consequences and give me another description.
GPT-4	<i>A new leather sofa sits amidst the chaos of the painting studio, its pristine surface untouched yet, but poised to become a tapestry of paint splashes and creative wear over time.</i>
User	Now, I want more paint on the sofa to make it look more messy. Consider the consequences and give me another description.
GPT-4	<i>A leather sofa in the painting studio, now splattered with a kaleidoscope of paint, stands as a messy yet vibrant testament to the bustling creativity that surrounds it.</i>

---

Table 3. Prompt used for prompting GPT-4 to generate a mechanistic description to reflect *Environmental Influence* for Stable Diffusion [49]. Note that the visual input is optional and the user can simply replace the given image with the scene prompt *a chaotic painting studio*. The user can give follow-up context (e.g., how long the leather sofa is placed, more versus less paint, etc.) to achieve more precise visual control.

---

**Prompting GPT-4 with optional visual input**

---

User [the scene]: the given image (or *a chaotic painting studio*)  
[the object]: *a leather sofa*

Now, imagine a picture where [the object] is placed into [the scene]. First, detailedly discuss the environmental impacts of [the scene] imposes on the appearance of [the object]. Focus on the physical impacts instead of lighting impacts.

Then provide a succinct instructions on how to change the appearance [the object] such that it looks realistic when placed in [the environment]. Start with each instruction with a verb and concatenate them with “;”. Aim the description to be approximately 20 to 30 words in length. Use simple language. Include all words provided in [the object].

User (optional)



GPT-4 Placing a leather sofa in the depicted artist’s studio, which is cluttered and has a very lived-in appearance, would result in a number of physical changes over time due to environmental factors present in the scene. The leather on the sofa would likely become discolored and faded due to exposure to sunlight streaming in from the large window. Dust and paint splatters could accumulate on its surface, given the messy nature of the studio. If the studio is frequently used, the leather might show signs of wear and tear, such as cracks or creases, particularly on the seat and armrests where the user would have the most contact. If there are any liquids like turpentine or oils used in the studio, they could cause stains or deterioration of the leather.

To make the leather sofa look realistic in this environment, the instructions would be: “Age the leather, fade the color, add dust layers, simulate paint splatters, incorporate wear marks, show creases, and place stains strategically.”

---

Table 4. Prompt used for prompting GPT-4 to generate a succinct instruction to reflect *Environmental Influence* for InstructPix2Pix [3]. Note that the visual input is optional and the user can simply replace the given image with the scene prompt *a chaotic painting studio*.

## References

- [1] <https://polyhaven.com>. 4, 12
- [2] Naofumi Akimoto, Yuhi Matsuo, and Yoshimitsu Aoki. Diverse plausible 360-degree image outpainting for efficient 3dcg background creation. In *CVPR*, 2022. 7
- [3] Tim Brooks, Aleksander Holynski, and Alexei A. Efros. Instructpix2pix: Learning to follow image editing instructions. In *CVPR*, 2023. 3, 10, 11, 16, 17, 18, 20
- [4] Tianshi Cao, Karsten Kreis, Sanja Fidler, Nicholas Sharp, and KangXue Yin. Textfusion: Synthesizing 3d textures with text-guided image diffusion models. In *ICCV*, 2023. 3, 11
- [5] Bor-Chun Chen and Andrew Kae. Toward realistic image compositing with adversarial learning. In *CVPR*, 2019. 3
- [6] Dave Zhenyu Chen, Yawar Siddiqui, Hsin-Ying Lee, Sergey Tulyakov, and Matthias Nießner. Text2tex: Text-driven texture synthesis via diffusion models. *arXiv preprint arXiv:2303.11396*, 2023. 3, 11, 14
- [7] Rui Chen, Yongwei Chen, Ningxin Jiao, and Kui Jia. Fantasia3d: Disentangling geometry and appearance for high-quality text-to-3d content creation. In *ICCV*, 2023. 3, 4, 7, 8, 11, 12, 14, 15
- [8] Wenyan Cong, Li Niu, Jianfu Zhang, Jing Liang, and Liqing Zhang. Bargainnet: Background-guided domain translation for image harmonization. In *ICME*, 2021. 3
- [9] Wenyan Cong, Jianfu Zhang, Li Niu, Liu Liu, Zhixin Ling, Weiyan Li, and Liqing Zhang. Dovenet: Deep image harmonization via domain verification. In *CVPR*, 2020. 3
- [10] Matt Deitke, Dustin Schwenk, Jordi Salvador, Luca Weihs, Oscar Michel, Eli VanderBilt, Ludwig Schmidt, Kiana Ehsani, Aniruddha Kembhavi, and Ali Farhadi. Objaverse: A universe of annotated 3d objects. In *CVPR*, 2023. 4, 12
- [11] Youming Deng, Xueting Li, Sifei Liu, and Ming-Hsuan Yang. Dip: Differentiable interreflection-aware physics-based inverse rendering. *arXiv preprint arXiv:2212.04705*, 2022. 7
- [12] Prafulla Dhariwal and Alexander Nichol. Diffusion models beat gans on image synthesis. *NeurIPS*, 2021. 8
- [13] Ainaz Eftekhari, Alexander Sax, Jitendra Malik, and Amir Zamir. Omnidata: A scalable pipeline for making multi-task mid-level vision datasets from 3d scans. In *ICCV*, 2021. 7
- [14] Rinon Gal, Yuval Alaluf, Yuval Atzmon, Or Patashnik, Amit H. Bermano, Gal Chechik, and Daniel Cohen-Or. An image is worth one word: Personalizing text-to-image generation using textual inversion, 2022. 10
- [15] Jun Gao, Tianchang Shen, Zian Wang, Wenzheng Chen, Kangxue Yin, Daiqing Li, Or Litany, Zan Gojcic, and Sanja Fidler. Get3d: A generative model of high quality 3d textured shapes learned from images. *NeurIPS*, 2022. 3
- [16] Marc-André Gardner, Yannick Hold-Geoffroy, Kalyan Sunkavalli, Christian Gagné, and Jean-François Lalonde. Deep parametric indoor lighting estimation. In *ICCV*, 2019. 3, 12
- [17] Marc-André Gardner, Kalyan Sunkavalli, Ersin Yumer, Xiaohui Shen, Emiliano Gambaretto, Christian Gagné, and Jean-François Lalonde. Learning to predict indoor illumination from a single image. *arXiv preprint arXiv:1704.00090*, 2017. 3
- [18] Ian Goodfellow, Jean Pouget-Abadie, Mehdi Mirza, Bing Xu, David Warde-Farley, Sherjil Ozair, Aaron Courville, and Yoshua Bengio. Generative adversarial nets. *NeurIPS*, 2014. 3
- [19] Jiatao Gu, Alex Trevithick, Kai-En Lin, Joshua M Susskind, Christian Theobalt, Lingjie Liu, and Ravi Ramamoorthi. Nerfdiff: Single-image view synthesis with nerf-guided distillation from 3d-aware diffusion. In *ICML*, 2023. 14
- [20] Roy Hachnouchi, Mingrui Zhao, Nadav Orzech, Rinon Gal, Ali Mahdavi-Amiri, Daniel Cohen-Or, and Amit Haim Bermano. Cross-domain compositing with pretrained diffusion models. *arXiv preprint arXiv:2302.10167*, 2023. 2, 3, 7, 8
- [21] Ayaan Haque, Matthew Tancik, Alexei Efros, Aleksander Holynski, and Angjoo Kanazawa. Instruct-nerf2nerf: Editing 3d scenes with instructions. In *CVPR*, 2023. 3, 17
- [22] Jonathan Ho, Ajay Jain, and Pieter Abbeel. Denoising diffusion probabilistic models. *NeurIPS*, 2020. 2, 3
- [23] Jonathan Ho and Tim Salimans. Classifier-free diffusion guidance. *NeurIPS*, 2021. 4, 5, 12, 16, 17, 18
- [24] Yannick Hold-Geoffroy, Akshaya Athawale, and Jean-François Lalonde. Deep sky modeling for single image outdoor lighting estimation. In *CVPR*, 2019. 3, 7
- [25] Yannick Hold-Geoffroy, Kalyan Sunkavalli, Sunil Hadap, Emiliano Gambaretto, and Jean-François Lalonde. Deep outdoor illumination estimation. In *CVPR*, 2017. 3
- [26] Wenzel Jakob, Sébastien Speierer, Nicolas Roussel, and Dario Vicini. Dr.jit: A just-in-time compiler for differentiable rendering. *TOG*, 2022. 3, 12, 17
- [27] Wenzel Jakob, Sébastien Speierer, Nicolas Roussel, and Dario Vicini. Dr.jit: A just-in-time compiler for differentiable rendering. *TOG*, 2022. 12
- [28] Yifan Jiang, He Zhang, Jianming Zhang, Yilin Wang, Zhe Lin, Kalyan Sunkavalli, Simon Chen, Sohrab Amirghodsi, Sarah Kong, and Zhangyang Wang. Ssh: A self-supervised framework for image harmonization. In *ICCV*, 2021. 3
- [29] Hiromichi Kamata, Yuiko Sakuma, Akio Hayakawa, Masato Ishii, and Takuya Narihira. Instruct 3d-to-3d: Text instruction guided 3d-to-3d conversion. *arXiv preprint arXiv:2303.15780*, 2023. 3, 17
- [30] Mohammad Reza Karimi Dastjerdi, Jonathan Eisenmann, Yannick Hold-Geoffroy, and Jean-François Lalonde. Everlight: Indoor-outdoor editable hdr lighting estimation. In *ICCV*, 2023. 3, 7
- [31] Mohammad Reza Karimi Dastjerdi, Yannick Hold-Geoffroy, Jonathan Eisenmann, Siavash Khodadadeh, and Jean-François Lalonde. Guided co-modulated GAN for 360 field of view extrapolation. *3DV*, 2022. 3
- [32] Chen-Hsuan Lin, Jun Gao, Luming Tang, Towaki Takikawa, Xiaohui Zeng, Xun Huang, Karsten Kreis, Sanja Fidler, Ming-Yu Liu, and Tsung-Yi Lin. Magic3d: High-resolution text-to-3d content creation. In *CVPR*, 2023. 3, 4
- [33] Minghua Liu, Chao Xu, Haian Jin, Linghao Chen, Zexiang Xu, Hao Su, et al. One-2-3-45: Any single image to 3d mesh in 45 seconds without per-shape optimization. *arXiv preprint arXiv:2306.16928*, 2023. 4

- [34] Andreas Lugmayr, Martin Danelljan, Andres Romero, Fisher Yu, Radu Timofte, and Luc Van Gool. Repaint: Inpainting using denoising diffusion probabilistic models. In *CVPR*, 2022. 8
- [35] Stephen McAuley, Stephen Hill, Naty Hoffman, Yoshiharu Gotanda, Brian Smits, Brent Burley, and Adam Martinez. Practical physically-based shading in film and game production. In *SIGGRAPH*. 2012. 4
- [36] Gal Metzer, Elad Richardson, Or Patashnik, Raja Giryes, and Daniel Cohen-Or. Latent-nerf for shape-guided generation of 3d shapes and textures. In *CVPR*, 2023. 3
- [37] Oscar Michel, Roi Bar-On, Richard Liu, Sagie Benaim, and Rana Hanocka. Text2mesh: Text-driven neural stylization for meshes. 2022. 3
- [38] Nasir Mohammad Khalid, Tianhao Xie, Eugene Belilovsky, and Tiberiu Popa. Clip-mesh: Generating textured meshes from text using pretrained image-text models. In *SIGGRAPH Asia*, 2022. 3
- [39] Jacob Munkberg, Jon Hasselgren, Tianchang Shen, Jun Gao, Wenzheng Chen, Alex Evans, Thomas Müller, and Sanja Fidler. Extracting triangular 3d models, materials, and lighting from images. In *CVPR*, 2022. 4
- [40] Michael Oechsle, Lars Mescheder, Michael Niemeyer, Thilo Strauss, and Andreas Geiger. Texture fields: Learning texture representations in function space. In *ICCV*, 2019. 3
- [41] OpenAI. Gpt-4 technical report, 2023. 5
- [42] Gaurav Parmar, Krishna Kumar Singh, Richard Zhang, Yijun Li, Jingwan Lu, and Jun-Yan Zhu. Zero-shot image-to-image translation. In *SIGGRAPH*, 2023. 5
- [43] Ben Poole, Ajay Jain, Jonathan T Barron, and Ben Mildenhall. Dreamfusion: Text-to-3d using 2d diffusion. *ICLR*, 2023. 2, 3, 4, 13
- [44] Guocheng Qian, Jinjie Mai, Abdullah Hamdi, Jian Ren, Aliaksandr Siarohin, Bing Li, Hsin-Ying Lee, Ivan Skokhodov, Peter Wonka, Sergey Tulyakov, and Bernard Ghanem. Magic123: One image to high-quality 3d object generation using both 2d and 3d diffusion priors. *arXiv preprint arXiv:2306.17843*, 2023. 4
- [45] Alec Radford, Jong Wook Kim, Chris Hallacy, Aditya Ramesh, Gabriel Goh, Sandhini Agarwal, Girish Sastry, Amanda Askell, Pamela Mishkin, Jack Clark, et al. Learning transferable visual models from natural language supervision. In *ICML*, 2021. 3
- [46] Aditya Ramesh, Mikhail Pavlov, Gabriel Goh, Scott Gray, Chelsea Voss, Alec Radford, Mark Chen, and Ilya Sutskever. Zero-shot text-to-image generation. In *ICML*, 2021. 2
- [47] René Ranftl, Katrin Lasinger, David Hafner, Konrad Schindler, and Vladlen Koltun. Towards robust monocular depth estimation: Mixing datasets for zero-shot cross-dataset transfer. *PAMI*, 2022. 7
- [48] Elad Richardson, Gal Metzer, Yuval Alaluf, Raja Giryes, and Daniel Cohen-Or. Texture: Text-guided texturing of 3d shapes. *SIGGRAPH*, 2023. 3, 4, 7, 8, 11, 14, 15
- [49] Robin Rombach, Andreas Blattmann, Dominik Lorenz, Patrick Esser, and Björn Ommer. High-resolution image synthesis with latent diffusion models, 2021. 2, 3, 4, 5, 19
- [50] Chitwan Saharia, William Chan, Saurabh Saxena, Lala Li, Jay Whang, Emily L Denton, Kamyar Ghasemipour, Raphael Gontijo Lopes, Burcu Karagol Ayan, Tim Salimans, et al. Photorealistic text-to-image diffusion models with deep language understanding. *NeurIPS*, 2022. 2, 3
- [51] Tianchang Shen, Jun Gao, Kangxue Yin, Ming-Yu Liu, and Sanja Fidler. Deep marching tetrahedra: a hybrid representation for high-resolution 3d shape synthesis. *NeurIPS*, 2021. 12
- [52] Yawar Siddiqui, Justus Thies, Fangchang Ma, Qi Shan, Matthias Nießner, and Angela Dai. Texturify: Generating textures on 3d shape surfaces. In *ECCV*, 2022. 3
- [53] Yang Song, Jascha Sohl-Dickstein, Diederik P Kingma, Abhishek Kumar, Stefano Ermon, and Ben Poole. Score-based generative modeling through stochastic differential equations. In *ICLR*, 2021. 3
- [54] Yizhi Song, Zhifei Zhang, Zhe Lin, Scott Cohen, Brian Price, Jianming Zhang, Soo Ye Kim, and Daniel Aliaga. Object-stitch: Generative object compositing. *CVPR*, 2023. 2, 3
- [55] Christina Tsalicoglou, Fabian Manhardt, Alessio Tonioni, Michael Niemeyer, and Federico Tombari. Textmesh: Generation of realistic 3d meshes from text prompts. 2024. 3
- [56] Narek Tumanyan, Michal Geyer, Shai Bagon, and Tali Dekel. Plug-and-play diffusion features for text-driven image-to-image translation. In *CVPR*, 2023. 5
- [57] Bruce Walter, Stephen R Marschner, Hongsong Li, and Kenneth E Torrance. Microfacet models for refraction through rough surfaces. In *EGSR*, 2007. 4
- [58] Haochen Wang, Xiaodan Du, Jiahao Li, Raymond A Yeh, and Greg Shakhnarovich. Score jacobian chaining: Lifting pretrained 2d diffusion models for 3d generation. In *CVPR*, 2023. 2, 3
- [59] Zhengyi Wang, Cheng Lu, Yikai Wang, Fan Bao, Chongxuan Li, Hang Su, and Jun Zhu. Prolificdreamer: High-fidelity and diverse text-to-3d generation with variational score distillation. *NeurIPS*, 2023. 3, 4, 7, 8, 11, 12, 13, 14, 15
- [60] Li-Yi Wei, Sylvain Lefebvre, Vivek Kwatra, and Greg Turk. State of the art in example-based texture synthesis. *EG-STAR*, 2009. 3
- [61] Jianxiong Xiao, Krista A Ehinger, Aude Oliva, and Antonio Torralba. Recognizing scene viewpoint using panoramic place representation. In *ICCV*, 2012. 3
- [62] Chun-Han Yao, Amit Raj, Wei-Chih Hung, Yuanzhen Li, Michael Rubinstein, Ming-Hsuan Yang, and Varun Jampani. Artic3d: Learning robust articulated 3d shapes from noisy web image collections. *arXiv preprint arXiv:2306.04619*, 2023. 14
- [63] Jinsong Zhang, Kalyan Sunkavalli, Yannick Hold-Geoffroy, Sunil Hadap, Jonathan Eisenman, and Jean-François Lalonde. All-weather deep outdoor lighting estimation. In *CVPR*, 2019. 3